Selective Partial Hydrogenation of Acrolein on Pd: a Mechanistic Study

Karl-Heinz Dostert[1], Casey P. O'Brien[1], Francesca Mirabella,[1] Francisco Ivars-Barceló ,[1] Smadar Attia,[1] Evan Spadafora,[1] Swetlana Schauermann[1,2,], and Hans-Joachim Freund[1]*

[1]Fritz-Haber-Institut der Max-Planck-Gesellschaft, Faradayweg 4-6, 14195 Berlin, Germany

[2]Institut für Physikalische Chemie, Christian-Albrechts-Universität zu Kiel, Max-Eyth-Str. 2, 24118 Kiel, Germany

Abstract

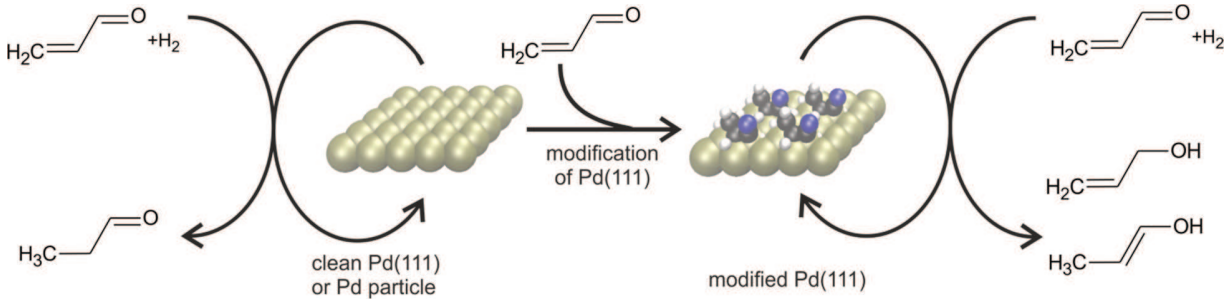

Identifying the surface processes governing the selectivity in hydrogenation of α,β-unsaturated carbonyl compounds on late transition metals is crucial for the rational design of new catalytic materials with the desired selectivity towards C=C or C=O bond hydrogenation. The partial selective hydrogenation of acrolein on a Pd(111) single crystal and Fe_3O_4-supported Pd nanoparticles under well-defined UHV conditions was investigated in the present study as a prototypical reaction. Molecular beam techniques were combined with infrared reflection-absorption spectroscopy (IRAS) and quadrupole mass spectrometry (QMS) in order to simultaneously monitor the evolution of surface species and the formation of the final gas-phase products under the isothermal reaction conditions as a function of surface temperature. Over a Pd(111) single crystal, acrolein is hydrogenated at the C=O bond to form the desired reaction product propenol with nearly 100% selectivity in the temperature range between 250 and 300 K,

while over Pd/Fe_3O_4, selective hydrogenation of the C=C bond to form propanal occurs. We found that the exceptionally high selectivity towards C=O bond hydrogenation over Pd(111) is connected to the initial modification of the catalytic surface with a dense monolayer of an oxopropyl surface species. This strongly bound oxopropyl layer is formed on the pristine Pd crystal in the induction period from half-hydrogenation of the C=C bond in acrolein. Subsequently deposited acrolein molecules adsorb via the C=O bond and form a half-hydrogenated reaction intermediate propenoxy species, which is attached to Pd via the C-O single bond. The evolution of the surface concentration of the propenoxy intermediate monitored spectroscopically was found to closely follow the propenol formation rate detected in the gas phase. At temperatures higher than 300 K on Pd(111) and on Pd nanoparticles supported on Fe_3O_4, decarbonylation of acrolein occurs leading to accumulation of CO and strongly dehydrogenated carbonaceous species on the surface. This process prevents formation of well-ordered overlayers of oxopropyl species required for selective C=O bond hydrogenation resulting in only minor non-selective hydrogenation of acrolein. At temperatures below 250 K on Pd(111), only a small fraction of the initially adsorbed acrolein is converted into the oxopropyl species yielding a partially modified surface and thus rather unselective formation of both products propanal and propenol.

Introduction

Selective partial hydrogenation of multi-unsaturated hydrocarbons, such as α,β-unsaturated aldehydes and ketones is of broad interest for numerous industrial applications. The production of unsaturated alcohols from selective hydrogenation of the C=O bond in unsaturated carbonyl compounds is particularly desired in the field of fine chemicals and pharmaceuticals [1]. Thermodynamics, however, favors hydrogenation of the C=C bond to form the saturated aldehyde by about 35 kJ/mol [1b]. Hence, production of unsaturated alcohols requires manipulation of the reaction kinetics by suitable catalysts. In previous studies on powdered supported catalysts, a variety of metals, including Pt, Pd, Rh, Ni, Cu, Ag, and Au, have been investigated to understand and improve the activity and selectivity of this reaction. [1a-2] Particularly over Pt group metals, the undesired hydrogenation of the C=C bond in α,β-unsaturated aldehydes is strongly favored over the desired C=O bond hydrogenation with the selectivity close to 100%. The amount of steric hindrance to adsorption via the C=C bond,[3] alloying with other metals[4] and addition of surface

modifiers[5] have been identified as key structural parameters controlling the chemoselectivity. The selectivity to C=O bond hydrogenation can be increased by using aldehydes or ketones with sterically shielded C=C groups, e.g. prenal instead of acrolein [3, 6]. In another approach, partially reducible supports like TiO_2 were used to provide Lewis-acid sites which are believed to coordinate and thus activate the C=O bond. [7].

Complementary, a large body of theoretical work and mechanistic experimental studies on well-defined single crystal surfaces have been reported, in which the factors governing the chemoselectivity of this process are addressed.[8] Despite these efforts, the problem of the selective hydrogenation of a carbonylic group in α,β-unsaturated aldehydes and ketones remains unsolved, especially for the smallest molecule (acrolein) having no protective groups close to the C=C bond. Also the nature of the reaction intermediates formed on a catalytic surface under the reaction conditions is not fully understood. This atomistic-level information on the underlying surface chemistry is crucial to approach rational design of selective catalysts for this class of reactions.

In our recent study, we investigated the partial selective hydrogenation of acrolein on a Pd(111) single crystal and on Pd nanoparticles supported over Fe_3O_4 model catalysts.[9] Figure 1 shows two possible reaction pathways of acrolein partial hydrogenation leading to hydrogenation of either C=C or C=O bonds to form propanal or propenol, respectively. We have shown that acrolein can be hydrogenated to the unsaturated alcohol (propenol) with nearly 100% selectivity over Pd(111). However, this surface requires a modification with a dense overlayer of oxopropyl species that are formed in the induction period of the reaction by half-hydrogenation of the C=C bond in acrolein. The steric constrain induced by this densely packed surface species turns the surface highly selective toward C=O bond hydrogenation.

In the present study, we use a combination of molecular beam techniques with infrared reflection-absorption spectroscopy (IRAS) and quadrupole mass spectrometry (QMS) to systematically investigate this reaction under isothermal reaction conditions in a broad temperature range. The particular focus lies on identification of the surface species formed under the reaction conditions, both the reaction intermediates and the spectator species, as well as the adsorbates poisoning the surface, and monitoring their formation and evolution as a function of surface temperature. Towards this goal, we simultaneously monitored the evolution of the adsorbates formed on the catalyst surface and the formation of reaction products in the gas phase. It was found

that formation of different adsorbates, including the oxopropyl species crucial for enhanced selectivity, strongly depends on the surface temperature. At 270 K a dense layer of oxopropyl species was observed on Pd(111) that turns the surface highly selective and allows formation of the propenoxy reaction intermediate, which can be further converted to the desired product propenol. Below 250 K, formation of the oxopropyl overlayer required for selective hydrogenation is most likely kinetically hindered, resulting in only partial modification of the surface and low activity and selectivity towards propenol. Above 300 K, acrolein shows a high degree of decomposition on Pd(111) leading to accumulation of CO and strongly dehydrogenated carbonaceous deposits, which block the surface and prevent chemoselective chemistry. A similar scenario was observed on Pd nanoparticles: acrolein strongly decomposes to CO and carbonaceous deposits and shows only very minor activity in the whole investigated temperature range.

Experimental Details

All experiments have been performed at the Fritz-Haber-Institut, Berlin, in a UHV apparatus that has been described in detail previously [10]. In brief, acrolein and H_2 have been dosed onto the sample through two doubly differentially pumped multi-channel array sources controlled by valves and shutters. The sources have been operated at room temperature, and the beam diameter has been chosen to exceed the sample size. The Pd(111) single crystal was cleaned prior to use by repeated cycles of Ar^+ ion bombardment at room temperature, annealing at 1000 K and oxidation in $1 \cdot 10^{-6}$ mbar O_2 at 750 K to remove residual carbon. The final cleaning cycle was stopped after annealing. The flatness and cleanliness of the Pd(111) single crystal surface was checked by low-energy electron diffraction (LEED) and infrared reflection-absorption spectroscopy (IRAS) of adsorbed CO. The Pd/Fe_3O_4 model catalysts were prepared as follows: the thin (≈100 Å) Fe_3O_4 film was grown on a Pt(111) single crystal surface by repeated cycles of Fe (≥ 99.99%, Goodfellow) physical vapor deposition and subsequent oxidation [10-11]. The quality of the oxide film was checked by LEED. Pd particles (≥ 99.9%, Goodfellow) were grown by physical vapor deposition using a commercial evaporator (Focus, EFM3, flux calibrated by a quartz microbalance) while keeping the sample temperature fixed at 115 K. The Pd coverage used in these experiments was 7 Å. The quality of the Pd particles has been investigated by IRAS after adsorption of CO. During Fe or Pd evaporation the sample has been biased to the same potential as the evaporant in the evaporator

(850 V) in order to avoid the creation of defects by metal ions. The resulting surfaces have been annealed to 600 K, and stabilized via cycles of oxygen ($8 \cdot 10^{-7}$ mbar for 1000 s) and CO ($8 \cdot 10^{-7}$ mbar for 3000 s) exposures at 500 K until the Pd particles reached a stable geometry with 12 nm in diameter [12].

IRAS data have been acquired using a vacuum Fourier-Transform Infrared (FT-IR) spectrometer (Bruker IFS 66v/S) with a spectral resolution of 2 cm^{-1} and a mid-infrared (MIR) polarizer and p-polarized IR light. An automated quadrupole mass spectrometer (QMS) system (ABB Extrel) has been employed for the continuous monitoring of the partial pressures of the reactants (acrolein: parent ion at 56 amu; H_2: at 2 amu) and products (propanal: parent ion and main fragment at 58 amu; propenol: parent ion at 58 amu, main fragment at 57 amu; further fragment at 31 amu; propanol: parent ion 60 amu, main fragment at 31 amu). It is difficult to unambiguously distinguish between the two possible forms of propenol – allyl alcohol (1-propen-3-ol) and the enol (1-propen-1-ol) – by mass spectrometry. Therefore, we do not specify the propenol species in more detail.

Shortly before each experiment the sample was flashed to 600 K before cooling to the desired temperature. In all experiments, the sample was pre-exposed to H_2 with a constant flux of $4.8 \cdot 10^{15}$ molecules/($cm^2 \cdot s$) for 5 min before exposure to acrolein with a constant flux of $1.5 \cdot 10^{13}$ molecules/($cm^2 \cdot s$). To improve the resolution of IR spectra in the course of acrolein conversion, additional IRAS measurements were performed with a reduced acrolein flux of $0.6 \cdot 10^{13}$ molecules/($cm^2 \cdot s$). Acrolein (Fluka, 95% purity) was purified prior to the experiments by repeated freeze-pump-thaw cycles.

The modification of Pd surface sites before the onset of the product formation was investigated by IRAS measurements after CO exposure. Acrolein was dosed together with H_2 until the onset of the product formation after 24 s. The sample was then cooled to 120 K and exposed to $9 \cdot 10^{15}$ CO molecules/cm^2.

Results and Discussion

Acrolein partial hydrogenation on Pd(111) in the 220–350 K temperature range

In order to understand how the surface temperature affects the selectivity, acrolein hydrogenation was investigated on a Pd(111) single crystal under isothermal reaction conditions in the 220-350 K temperature range . Prior each experiment, the Pd(111) surface was pre-exposed to $4.8 \cdot 10^{15}$ H_2 molecules$\cdot cm^{-2}$ during 300 s before the acrolein beam with the flux $1{,}5 \cdot 10^{13}$ molecules$\cdot cm^{-2} \cdot s^{-1}$ was switched on. Starting from this point, both beams were operated in a continuous mode.

Figure 2 shows the propanal and propenol formation rates detected in the gas phase by quadrupole mass spectrometry at seven different temperatures in the 220-350 K temperature range. The time scale was chosen such that acrolein exposure starts at time zero. No full hydrogenation to propanol was observed ar any of the investigated temperatures.

While the amount of propanal detected in the gas phase is rather small at all investigated temperatures, the propenol formation rate exhibits a clear temperature dependence with a strong maximum near 270 K. The full dataset can be tentatively divided into three reactivity regimes: low activity and selectivity below 250 K, high activity and selectivity between 250 and 300 K and the regime of low activity and selectivity above 300 K.

At the temperatures 220 and 235 K, small amounts of both products successively appear with propanal evolving first at the beginning of acrolein exposure followed by formation of propenol. The formation rate of propanal passes through a maximum after about 20 s and subsequently decreases to zero. The propenol rate increases more slowly, reaches a maximum after 50 s and then declines to zero after about 120 s.

In the intermediate temperature range 250-300 K, the Pd(111) surface is highly active and selective for propenol formation. Nearly 100% selectivity towards propenol formation is observed at 250 and 270 K, while it slightly decreases at 300 K. In this temperature range the reaction shows a clear induction period: while essentially no propenol can be detected in the gas phase within the first few tens of seconds of acrolein exposure, the reaction rate strongly increases after this period and reaches a maximum after about 100 s before slowly declining. At 250 K and 270 K, the induction period is 20-24 s, long while it extends to 48 s at 300 K. The formation rate of propenol

at the maximum exceeds by more than an order of magnitude th rate at 220 K. Only negligible propanal formation rate could be observed during the entire reaction.

By using molecular beam techniques with the known absolute acrolein flux, we can estimate the amount of acrolein molecules accommodated on the surface during the induction period. At 270 K, about $3.6 \cdot 10^{14}$ acrolein molecules$\cdot cm^{-2}$ are accommodated at the surface prior the onset of the propenol formation rate. This amount corresponds to accumulation of approximately one molecule of acrolein (or acrolein derivative) per four Pd surface atoms or to a formal coverage of 0,25 ML of acrolein derivatives as referred to the number of surface Pd atoms. With this, a rather densely packed overlayer of acrolein derivatives is formed prior the onset of propenol formation and desorption into the gas phase.

At temperatures above 300 K, both propanal and propenol are formed in small quantities at similar reaction rates. Propanal appears in the gas phase after an induction period of about 20 s and propenol formation is detected after an induction period of about 30 s. The formation rates of both products go through a maximum at 40 s and then decrease to zero. At temperatures above 320K, no productscould be observed.

The observed temperature and time dependence of the reaction rates suggest a complex interplay between multiple surface processes, crucially affecting the activity and selectivity. In order to get deeper atomistic level understanding of the observed phenomena, we followed the evolution of gas-phase products and the surface species using IRAS simultaneously. The results are discussed in the following sections. First we will focus on the intermediate temperature regime with the highest activity and selectivity towards propenol formation followed by the discussion of the lower and higher temperature regimes characterized by lower activity and selectivity.

Acrolein Conversion on Pd(111) at 270 K

The time dependence of the propenol formation rate at 270 K shown in Figure 2 suggests three reactivity regimes: *(i)* an induction period at the beginning of the reaction when acrolein is accumulated on the surface but no propenol is formed; *(ii)* the period of highest activity and

selectivity towards propenol formation and *(iii)* deactivation of the catalysts leading to a slow decrease of the reaction rate.

In order to study the structural changes occurring during the induction period, the Pd(111) surface was exposed to both reactants for 24 s at 270 K, then the surface was cooled down to 120 K and IR spectra of CO were recorded to spectroscopically probe the availability of free adsorption sites. Figure 3a shows the onset of the induction period indicated with an arrow. The IR spectrum obtained on this surface after interruption of the reaction just after the induction period is displayed in Figure 3b (black line) together with the IR spectrum of CO recorded on pristine Pd(111) (grey line) shown for comparison. While on the clean surface a strong IR absorption peak related to the C–O stretching vibration is observed, no CO-related vibrations could be detected on the Pd surface covered with the acrolein derivatives formed during the induction period. This observation suggests that the adsorbed hydrocarbons must be rather homogeneously distributed over the entire surface than accumulated in islands, as in latter case some CO should be able to adsorb in the free metal patches.

Identification of the surface species formed under the reaction conditions

The nature of the surface species formed on Pd(111) under reaction conditions at 270 K was investigated by IRAS. Figure 4 shows three representative IR spectra obtained in the three reactivity regimes on the surface turning over. The second spectrum from top was obtained on the surface during the first 45 s (total acrolein exposure $6.8 \cdot 10^{14}$ molecules/cm^2), comprising the induction period and the period of growing reactivity. The third spectrum was recorded during the next 45 s (from 45 to 90 s after the beginning of acrolein exposure, total acrolein exposure $13.6 \cdot 10^{14}$ molecules/cm^2), corresponding to the high propenol formation rates. The bottom spectrum (4) shows the composition of the deactivated surface at the end of the experiment (obtained between 450 and 540 s, acrolein total exposure $7{,}4 \cdot 10^{15}$ molecules/cm^2). In these spectra, three spectral regions characteristic for the CH_x stretching vibrations (3200–2700 cm^{-1}), C=O and C=C stretching vibrations (1850-1550 cm^{-1}), and CH_x deformation as well as C–O and C–C stretching vibrations ($\leq$ 1500 cm^{-1}) can be distinguished.

For comparison, the IR spectrum of an acrolein monolayer adsorbed on Pd(111) at 100 K, which was obtained after exposure of $3.6 \cdot 10^{14}$ acrolein molecules$\cdot$cm^{-2}, is displayed at the top of Figure 4. At this temperature, acrolein does not react and adsorbs molecularly on Pd. The spectrum of molecularly adsorbed acrolein was discussed in detail previously. [9, 13] Briefly, the most pronounced band appears at 1663 cm^{-1}, which can be related to the stretching vibration of the carbonyl (C=O) group that is conjugated to the C=C group, with a less-pronounced band in the 1430-1400 cm^{-1} range, which is assigned to a scissor deformation of the methylene (CH_2) group.

The spectrum (2) in Figure 4 obtained during the induction period and the period of growing reactivity is clearly different from that of molecularly adsorbed acrolein. A pronounced IR vibrational mode appears at 1755 cm^{-1} and a second one near 1120 cm^{-1}. The vibration at 1755 cm^{-1} which is blue-shifted by 92 cm^{-1} relative to the carbonyl band in acrolein, is typical for the carbonyl stretching mode in saturated aldehydes and ketones[14], and is associated with a C=O stretching vibration that is not conjugated to a C=C group. The appearance of this new vibration under reaction conditions points to the formation of an oxopropyl surface species, resulting from partial hydrogenation of the C=C group in acrolein with only one H atom. Our data do not allow to make a more precise conclusion on whether acrolein has been hydrogenated on the α or β C atom to form this species; both products would be consistent with the IR vibration at 1755 cm^{-1}. One of two possible structures of this adsorbate is shown on the right of Figure 4. In the course of the reaction, the intensity of the vibrational band at 1755 cm^{-1} grows and later saturates (see spectra 3 and 4), even when the reaction rate of propenol formation in the gas phase decreases to zero. From this it can be concluded that the oxopropyl species is not the direct reaction intermediate for propenol formation but rather a spectator species. In the following, we will refer to it as to the spectator species S1.

The band at 1120 cm^{-1} appears during the first 45 s of acrolein exposure (spectrum (2) in Figure 4) and becomes very pronounced in spectrum (3) obtained during the period of the highest propenol formation rates (45 s to 90 s). After the propenol formation rate decreases to zero, the intensity of this band also vanishes (spectrum (4)). Several other bands at 1090 cm^{-1}, 1463-1450 cm^{-1}, 2966 cm^{-1} and 2980 cm^{-1} follow a similar pattern as seen in Figure 4. This behavior shows that the evolution of the surface species associated with the band at 1120 cm^{-1} is strongly correlated with the formation rate of propenol detected in the gas phase.

The intense IR absorption features at 1090 cm^{-1} and 1120 cm^{-1} are present neither in adsorbed molecular acrolein on Pd nor in acrolein ice and therefore cannot be related to any distinctive vibration of an intact acrolein molecule. The vibration at 1120 cm^{-1} was previously assigned to a stretching mode of a saturated C–O bond, in which the oxygen atom is coordinated to a metal surface [13e, 15]. The IR absorption band at 1090 cm^{-1} can be assigned to a stretching vibration of a saturated C–C bond. In literature, C–C bond vibrations were reported in the range from about 1000 cm^{-1} to 1130 cm^{-1}, depending on their coordination to the surface [13b, 13e, 15f, 16] . The IR absorption at 1450 cm^{-1} to 1463 cm^{-1} appear in a range typical for CH_2 and CH_3 bending vibrations. Tentatively, we assign it to CH_3 asymmetric bending modes, which were reported in the range of 1450–1475 cm^{-1} [14a, 17]. Alternatively, it could also be related to a CH_2 scissor mode, which typically appear at slightly lower frequency near 1420-1430 cm^{-1} [13]. The vibrations at 2966 cm^{-1} and 2980 cm^{-1} can be clearly assigned to C–H stretching vibrations with the band at 2980 cm^{-1} being related to a C–H bond, in which the C atom is a part of an unsaturated C=C bond. [14a] In the region of C=O stretching vibrations, no IR absorption feature can be found that closely follows the evolution of the propenol formation rate. Also no O–H vibrations can be detected. Based on these observations, the structure of the reaction intermediate can be assigned to propenoxy species, which is the result of a half hydrogenation of acrolein on the C=O double bond. To form this reaction intermediate, one hydrogen atom attaches to the carbon atom in the C=O bond thus forming a saturated C–O bond with the vibrational frequency of 1120 cm^{-1}, in which O is coordinated to Pd atom in an η1-(O) configuration (CH_2=CH—CH_2—O—Pd). The C=C double bond is still preserved in the reaction intermediate as indicated by the C–H stretching frequency of 2980 cm^{-1} characteristic for a vynil group. Note that only one additional step – insertion of a second hydrogen atom into the O–Pd bond is required to form the final reaction product propenol. In the following we will refer to this surface species as to the reaction intermediate (RI). Its proposed structure is shown in Figure 4. The high intensity of the band at 1120 cm^{-1}, exceeding even the most intense C=O vibrational band in acrolein and in the oxopropyl species (S1), additionally supports the formation of a C–O bond exhibiting a large dynamic dipole moment most likely due to the upright orientation of the propenoxy group.

It is important to note that the surface reaction intermediate is formed not on the pristine Pd(111) surface, but on the surface strongly modified with the oxopropyl spectator species (S1). Indeed, about one acrolein molecule per four Pd surface atoms is accumulated on Pd(111) to form

the spectator overlayer prior to the onset of propenol formation. Microscopically, this corresponds to a situation when every fourth Pd atom is covered by S1, forming a dense spectator overlayer structure. Most likely, a strong geometrical confinement imposed by the S1-covered surface on the available adsorption sites prevents acrolein adsorption via C=C bond, thus suppressing the competing pathway of C=C bond hydrogenation, and allows acrolein to adsorb only via the O atom to activate the C=O group. Obviously, the clean Pd(111) surface is not capable of activating the C=O group towards selective hydrogenation and the strong modification of the surface by S1 is required to trigger the desired selective chemistry.

The fourth IR spectrum in Figure 4 was collected after the formation rate of gas-phase propenol decreased almost to zero (between 450 s to 540 s). All features assigned to the half-hydrogenated intermediate RI (propenoxy species) are absent in spectrum (4). Instead, new vibrational bands are observed at 1330 cm^{-1}, 1375 cm^{-1}, in the range 2883–2892 cm^{-1} and at 2942 cm^{-1}. The sharp peak at 1330 cm^{-1} is characteristic for the umbrella bending mode of the CH_3 group in ethylidyne or ethylidyne-like species, which were observed in previous studies on Pd(111) and Pt(111).[18 20] The appearance of these new bands suggests that a fraction of acrolein decomposes in a decarbonylation reaction yielding a C_2 fragment (e.g. ethylidyne or ethylidine-like species) and probably a fragment containing a carbonyl group, which is in agreement with literature data.[19 14a, 14c] As deactivation of the catalyst occurs simultaneously with the appearance of ethylidyne-like species, it can be speculated that these decomposition products block the surface and stop the reaction.

Time resolved evolution of the reaction intermediate and the correlation with the formation rate of propenol.

In order to find detailed correlation between the evolution of the reaction intermediate RI on the surface and the appearance of propenol in the gas phase, IRAS studies with higher time resolution have been performed. Figure 5a shows a series of IR spectra obtained on the Pd(111) surface turning over at 270 K. During the acquisition of each spectrum the surface was exposed to $1.2 \cdot 10^{13}$ acrolein molecules/cm^2, which corresponds to 8 s of reaction time displayed in the time axis in Fgure 5b. Note that after the 6th spectrum only every fourth spectrum is shown in Figure 5a. Approximately in the 2nd or 3rd spectrum, the vibrations related to RI start to appear. The

intensities of the peaks grow until about the 7th to 8th spectrum following by disappearing all related features at the end of the reaction.

Figure 5b shows the gas-phase formation rate of propenol (grey line) together with the integral intensity of the most intense IR vibration band of the reaction intermediate RI at 1120 cm^{-1}, which can be assumed to approximately reflect the concentration of RI on the surface. It can be clearly seen that the evolution of the propenol formation rate in the gas phase closely follows the concentration of RI on the surface. Thus, the observed strong correlation unambiguously shows that the corresponding propenoxy surface species is a reaction intermediate that is directly involved in the selective hydrogenation of acrolein to the propenol.

Acrolein conversion in the low temperature range

Figure 2 shows that at 220 and 235 K only small amounts of both propenol and propanal are detected in the gas phase. To study the origin of the lower activity and selectivity at low temperatures we investigated the Pd(111) surface during the reaction at 220K by IRAS. Figure 6 shows a series of IR spectra obtained on this surface under the reaction conditions at 220 K (black) and at 270 K (grey) for comparison with a time resolution of 45 s per spectrum. The simultaneously detected formation rates of propanal and propenol at 220 K are shown on the right.

The weak IR band near 1750 cm^{-1} is the only band that appears in the whole series of IR spectra at 220 K. Its vibrational frequency is almost identical to that of the oxopropyl spectator species (S1) observed at 270 K, however, the intensity of this band is significantly smaller than at 270 K pointing to a much smaller concentration of oxopropyl adsorbates at 220K. This implies that only a rather small fraction of the Pd(111) surface is covered by S1 at 220 K. The reaction intermediate RI is not formed at 220 K as indicated by the absence of the peak at 1120 cm^{-1}. This observation is not surprising, as we have shown in the previous section that the reaction intermediate RI appears only on the surface covered with a densely packed overlayer of S1 species, which is not formed at 220 K. Since there is a small amount of propenol formed during the initial stages of the reaction, there is probably only very minor concentration of RI, which is below the detection level of our instrument. In contrast, the formation rate of propenal is significantly larger

than that observed at 270 K, pointing to more effective hydrogenation of the C=C bond at the S1-free surface. In total, the surface turning over at 220 K seems to consist of two regions – a rather small region modified with the spectator S1 species, which renders the surface highly selective to acrolein hydrogenation at the C=O bond to form propenol, and a significantly larger region, which is not covered by an ordered overlayer of the spectator species, at which C=C bond is preferentially hydrogenated to form propanal. The latter observation should mean that the second half-hydrogenation step in C=C bond hydrogenation (i.e. hydrogenation of the oxopropyl spectator species to propanal) is more effective at 220 K than at 270 K, which is rather surprising. This behavior can result likely from the different abundance of hydrogen on Pd – both on the surface and in the subsurface – at these two reaction temperatures as hydrogen desorbs much faster at 270 than at 220 K and can have therefore significantly lower steady state concentration under the reaction conditions.[20]

Acrolein conversion in the high temperature range.

Figure 2 shows that at temperatures above 300 K the activity and selectivity of the Pd catalyst in acrolein hydrogenation strongly decreases. We addressed the origins of this behavior by investigating the reaction at 320 K following the approach described above for lower temperatures.

Figure 7 shows series of time-resolved IR spectra obtained on the Pd(111) surface turning over at 320 K (black) and 270 K (grey) for comparison. The gas-phase formation rates of both products at 320 K are displayed on the right. During the first 45 s of acrolein exposure, two broad IR absorption features appear at 1850 cm^{-1} and 1800 cm^{-1} and a sharp peak can be observed at 1335 cm^{-1}. At the same time, the formation rates of both products increase and reach their maxima. In the following 45 seconds, the peak at 1850 cm^{-1} increases in intensity and shifts to 1880 cm^{-1}, and the peak at 1335 cm^{-1} becomes more intense. During this time, both product formation rates rapidly decrease from their maxima at 45 s to zero at reaction times greater than 90 s. After 90 seconds of reaction, only bands at 1880 cm^{-1} and 1335 cm^{-1} are observed and their intensity remains constant for the rest of the reaction. The bands observed in the 1800-1880 cm^{-1} range and their coverage dependence are typical for CO molecules adsorbed on Pd(111). [21] Note that vibrational spectra of CO are strongly affected by dipole coupling effects that result in significant intensity shifts and "intensity borrowing" effects at increasing coverage,[22] leading to non-linear

dependence of the peak intensity on the CO surface coverage. The IR vibration at 1335 cm^{-1} is indicative of ethylidyne (or ethylidyne-like species) formation, which was also observed at 270 K.

Based on the observed spectroscopic signatures, it can be concluded that – in contrast to lower temperatures – acrolein is nearly completely decomposed at 320 K to CO and ethylidyne. The surface saturates with these two species already after 45-90 s of acrolein exposure, which corresponds to the dose of $6.8 \cdot 10^{14}$-$1.4 \cdot 10^{15}$ acrolein molecules per cm^2. The minor hydrogenation rates to propanal and propenol were formed before the surface was saturated with CO and ethylidyne, indicating that the latter species are responsible for deactivation of the catalyst.

Our studies at 270 K already indicated that the products from acrolein decomposition are irreversibly accumulated on the surface and are responsible for the poisoning of the catalyst. At 270 K, however, the decomposition reaction was observed to occur to much lesser extent than at 320 as indicated by significantly lower intensities of the band at 1330 cm^{-1} associated with ethylidyne-like species. It is interesting to note that no significant amounts of molecular CO were detected at 270 K, probably pointing to a lesser extent of acrolein decomposition, e.g. to formation of aldehyde-like COH fragment showing the vibrational frequencies in the range, which is closer to the carbonyl vibration in oxopropyl species than to molecular CO. It is likely that this species is stable at the lower reaction temperature and does not further decompose to CO. It should also be taken into account that at temperatures near 320 K the hydrogen surface concentration is expected to be much lower than at 270 K due to the higher desorption rate[23]. A lower hydrogen concentration may further promote the decomposition of acrolein instead of the hydrogenation pathway.

Thus, our experimental results show that the lower activity and selectivity of Pd(111) at elevated temperatures results from the facile decarbonylation of acrolein to ethylidyne and CO that poison the catalyst's surface.

Acrolein hydrogenation over Pd nanoparticles supported on Fe_3O_4 at 270 K

In order to address the question of how the nanoscopic nature of supported powdered catalysis affects the selectivity in acrolein partial hydrogenation, we studied this reaction over model Pd nanoparticles supported on well-defined Fe_3O_4(111) film epitaxtially grown over Pt(111) single crystal. Here, we varied the particle size to follow the structure-reactivity relationships, which are discussed in detail elsewhere.[24] In this report, we will focus on the surface composition under the reaction conditions followed by IRAS and compare it to the results obtained on the extended Pd(111) surface described above.

Figure 8 shows the partial hydrogenation rates of acrolein to propanal and propenol measured over 12-nm sized Pd nanoparticles (left) and the vibrational spectra obtained on the surface turning over (right) at 270 K. In contrast to Pd(111), propanal was found to be the only gas-phase product formed on the Pd particles. The selective formation of propanal over Pd particles is in excellent agreement with earlier studies on high surface area powdered catalysts showing that only the C=C bond can be hydrogenated in acrolein [1b, 25]. The first IR spectrum was obtained during the first 20 seconds of acrolein exposure followed by the acquisition of the second spectrum in the next 20s; both spectra are related to the period of high propanal formation rate. The final spectrum was recorded after the reaction rate decreased to zero and the surface turned inactive. The IR spectra exhibit strong absorption bands in the range from 1800-1960 cm^{-1}, which can clearly be assigned to adsorbed molecular CO. Previously adsorption of CO was investigated on Pd nanoparticles of different sizes in detail.[26] Briefly, it can be distinguished between the CO molecules adsorbed on the regular (111) terraces (1800-1960 cm^{-1}) and the edges, corners and other low-coordinated surface sites of Pd nanoparticles, appearing as a sharp peak at appr. 1970 cm^{-1} The evolution of the vibrational bands in the range between 1800 and 1960 cm^{-1} during the reaction strongly suggest facile acrolein decarbonylation. It is interesting to note that the decarbonylation process occurs very effectively on Pd particles already at 270 K, while extended Pd(111) was shown to only slowly accumulate acrolein decomposition products and not being able to produce molecular CO. This difference in the decomposition behavior can be traced down to the presence of low-coordinated sites on Pd nanoparticles (edges, corners etc), which are more active than the (111) surface in decarbonylation of acrolein to produce CO.

Spectrum 3 in Figure 8 shows the surface composition of the catalyst after its complete deactivation (black) and a CO spectrum obtained on freshly prepared pristine Pd nanoparticles

plotted for comparison (grey). Both spectra show similar intensities in the range of CO vibrations at the regular (111) terraces (1800-1960 cm^{-1}), however, they strongly differ in the range characteristic for CO adsorbed at the particles edges. The band at 1970 cm^{-1}, which is associated with CO adsorbed on the edges and corners of Pd nanoparticles, is absent in the spectrum collected during the acrolein hydrogenation reaction, which indicates that the particle edges and corners are blocked for CO adsorption. It should be pointed out that the low coordinated sites are the strongest bonding sites for CO molecules[27], so that on the clean Pd nanoclusters CO should occupy these sites first. The observation made in our study that CO adsorbs on the (111) terraces but not at the edges means that these site are blocked to CO adsorption by some other adsorbates, which are even more strongly bound to the edges than CO. Such adsorbates could be the strongly dehydrogenated carbonaceous deposits (CH_x species) formed from acrolein, that were shown in our previous studies to preferentially adsorb at the edge sites.[28] As no ethylidyne-like species were detected on Pd nanoparticles as evidenced by the absence of the band at 1330 cm^{-1}, it can be concluded that the C_2-fragments resulting from acrolein decarbonylation quickly lose hydrogen atoms to form carbon or other strongly dehydrogenated CH_x species that preferentially occupy the edges of Pd nanoparticles and cannot be detected by IRAS.

Our results show that the opposite selectivity of acrolein hydrogenation on Pd nanoparticles and Pd(111) is related to significant differences in the surface chemistry under the reaction conditions. Since CO production on the Pd(111) crystal does not occur at 270 K, most likely the low-coordinated sites (edges, corners, (100) facets) of Pd nanoparticles catalyze acrolein decomposition to CO and strongly dehydrogenated carbonaceous, which prevents formation of the oxopropyl overlayer required for selective hydrogenation to propenol. Decarbonylation of acrolein to CO was also observed on the Pd(111) single crystal, however, only at significantly higher temperatures. IRAS spectra showing the preferential CO adsorption at the (111) facets of the nanoparticles indicate that CO rapidly diffuses to the (111) terraces while the CH_x fragments accumulate at the particle edges and corners. A model illustrating this scenario is shown in Figure 8.

Conclusions

In this study, the mechanistic details of the selective partial hydrogenation of acrolein over Pd under well-defined UHV conditions were investigated by employing molecular beam techniques combined with *in-situ* infrared spectroscopy. Well-defined Pd(111) single crystal surface and Pd nanoparticles supported on the model Fe_3O_4/Pt(111) film were used as catalysts.

In contrast to all previous studies on powdered Pd catalysts, where acrolein was reported to be hydrogenated almost exclusively on the C=C bond forming propanal, we found that the selective hydrogenation of the C=O bond with nearly 100% selectivity is possible over Pd(111).

By performing combined molecular beam and IRAS experiments, we identified the composition of the surface turning over in the range of the reaction conditions resulting in the highest activity and selectivity towards propenol formation. The selective hydrogenation of the C=O bond occurs only after the Pd(111) surface is modified by a dense layer of oxopropyl spectator species. This spectator species is formed from acrolein by adding one hydrogen atom to C=C bond during the initial stages of surface reaction and builds up a densely packed overlayer. By carrying out transient reactivity measurement combined with IRAS we were able to identify the chemical nature of the reactive surface intermediate as propenoxy species and experimentally follow the simultaneous evolution of the reactive intermediate on the surface and formation of the product in the gas phase. The reactive intermediate was found to form only on the surface covered by an overlayer of oxopropyl spectator species, most likely due to the geometrical constrain imposed on the adsorbing acrolein molecules. Simulateneously with hydrogenation, a slow decomposition process of acrolein occurs on this surface resulting in formation of ethylidyne or ethylidyne-like species that accumulate and finally deactivate the catalyst.

The highest activity and selectivity towards propenol formation was detected for the temperature 270 K. At lower and higher temperatures, different mechanisms were identified to be responsible for decreasing activity and selectivity of C=O bond hydrogenation.

In the low temperature range (220 – 235 K) only a small fraction of the initially adsorbed acrolein is converted to the oxopropyl species, and as a result, unselective formation of both products propanal and propenol occurs.

In the high temperature range (above 300 K), acrolein readily decomposes to CO and ethylidyne, which blocks the entire Pd surface and deactivates the catalyst. Before that point, unselective formation of both products at very slow rates could be observed.

Our studies on acrolein conversion over Pd nanoparticles supported on Fe_3O_4/Pt(111) model oxide films and Pd(111) at 270 K reveal a strong structural dependence of the selective partial hydrogenation. On Pd nanoparticles, fast acrolein decarbonylation to CO and probably some strongly dehydrogenated CH_x species occurs, which prevent formation of oxopropyl overlayer required for selective hydrogenation of C=O bond. The decomposition product were found to be inhomogeneously distributed over Pd nanoclusters with CO predominantly occupying the regular (111) terraces and CH_x species blocking the low-coordinated sites such as edges, corners etc. Those low-coordinated sites can be mostly responsible for facile acrolein decomposition preventing the desired reaction pathway to propenol.

Obtained atomistic-level insights into chemoselective hydrogenation chemistry of acrolein highlight the exceptional importance of spectator species which are usually formed on the catalytically active surface under reaction conditions. Related effects are expected to play a key role in controlling chemoselectivity in hydrogenation of all types of α,β-unsaturated aldehydes and ketones and hold great potential for further development of new selective powdered catalysts such as e.g. ligand-modified nanoparticles.

Acknowledgement

Support from the European Research Council (ERC Starting Grant ENREMOS, project number 335205) is gratefully acknowledged. S.S. thanks the Fonds der Chemischen Industrie for the Chemiedozentenstipendium.

Figures

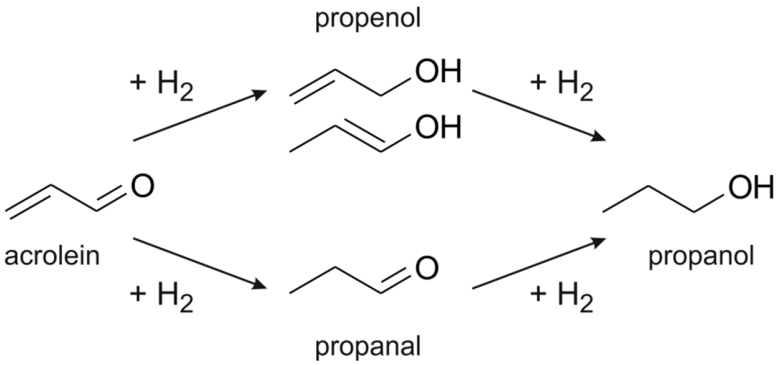

Figure 1: Possible reaction pathways of acrolein hydrogenation.

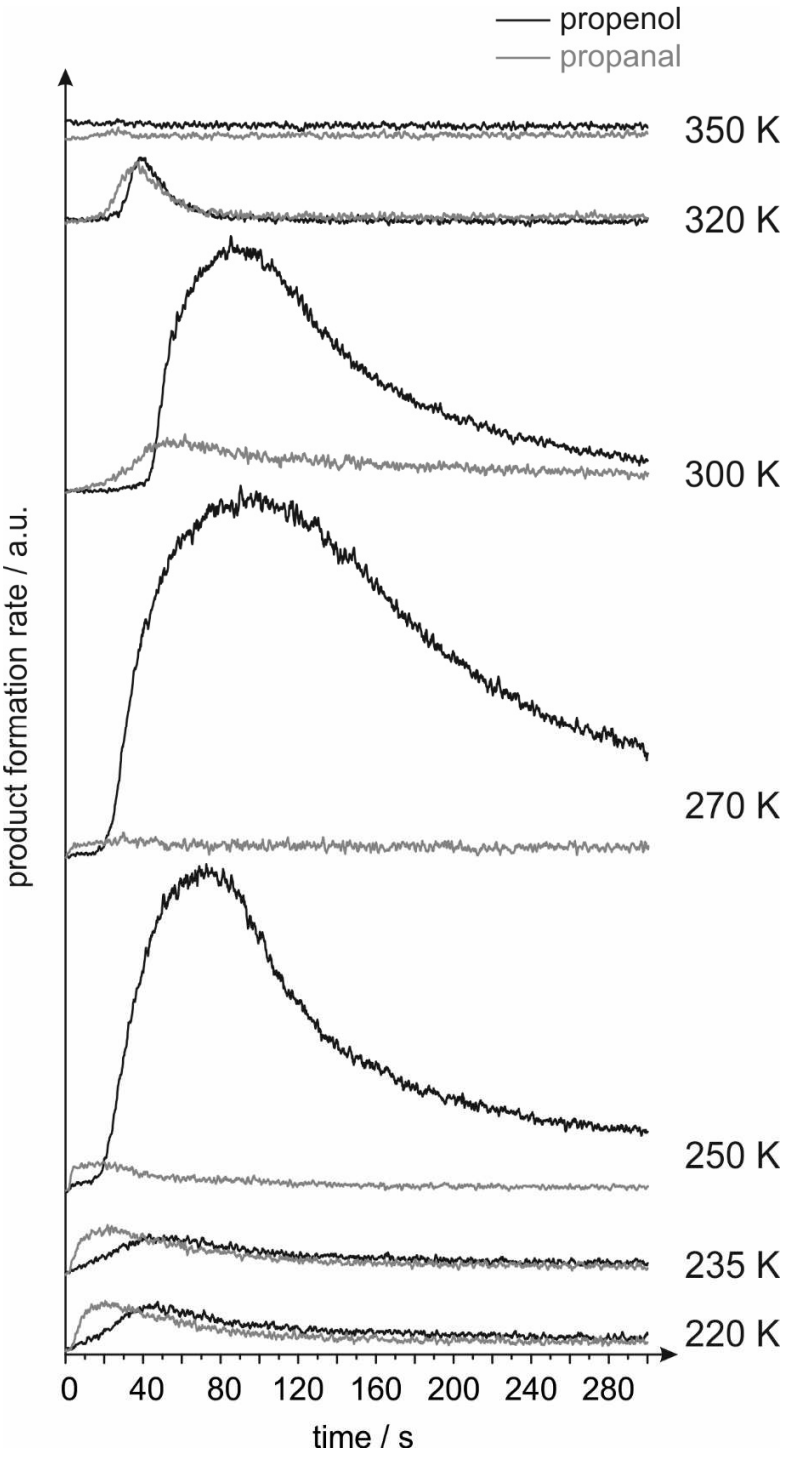

Figure 2: Formation rates of propenol (black) and propanal (grey) on Pd(111) during continuous exposure of acrolein and H_2 at different temperatures.

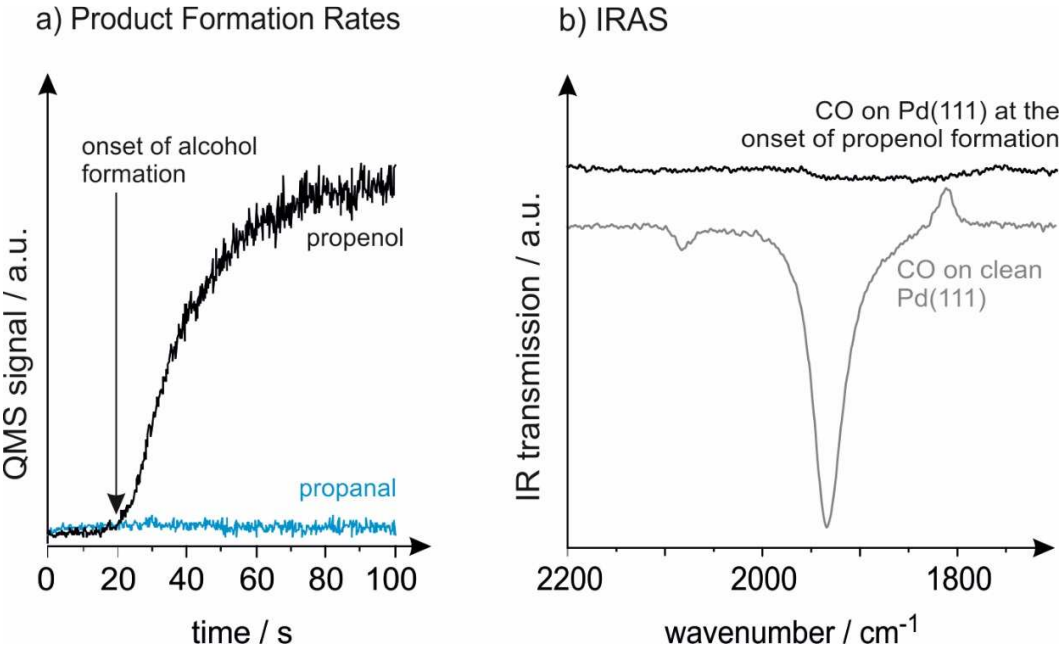

Figure 3: Formation rates of propenol (black) and propanal (blue) over Pd(111) at 270 K. Propenol formation starts after an induction period of appr. 20-24 s. (b) IR spectrum of CO adsorbed on a pristine Pd(111) surface (gray) and Pd(111) surface just after the onset of propenol formation (black). In the latter case the surface is completely blocked to CO adsorption.

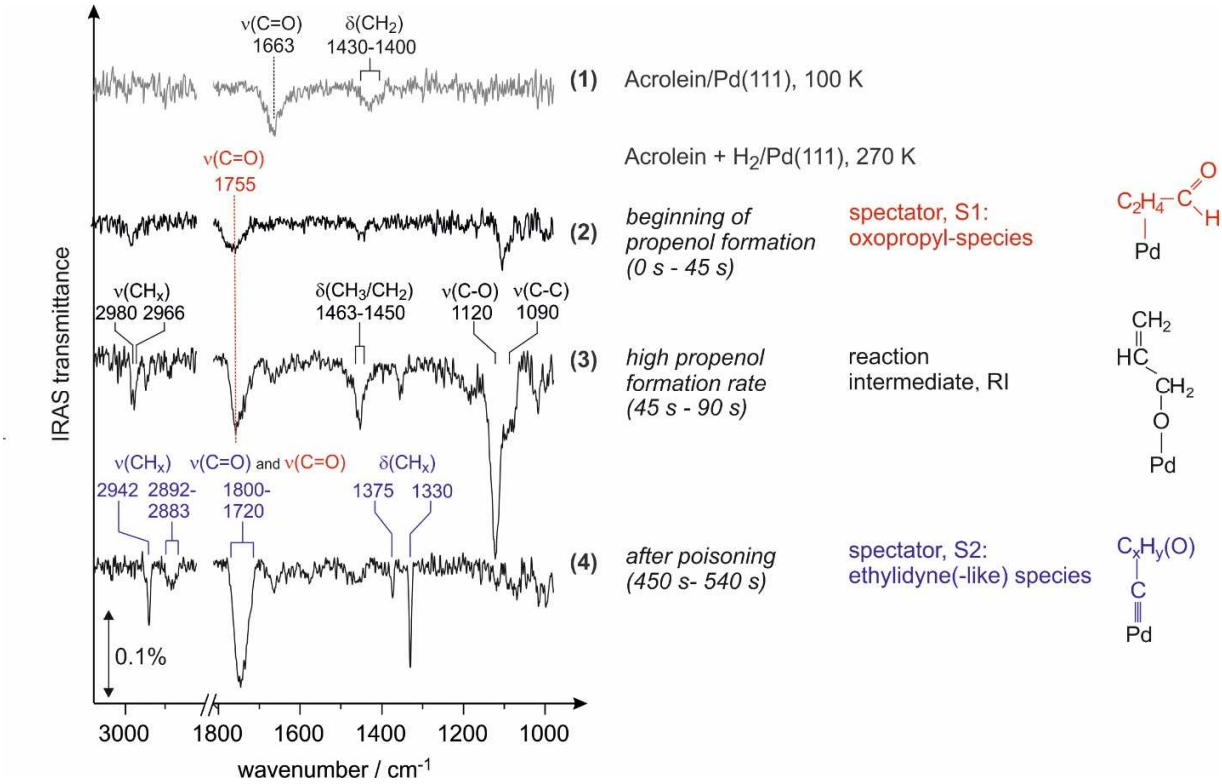

Figure 4: IR spectra of a monolayer of molecularly adsorbed acrolein on pristine Pd(111) at 100 K (grey trace, spectrum 1) and of the surface species formed on Pd(111) during continuous exposure to acrolein and H_2 at 270 K(black traces, spectra 2-4). The second spectrum 2 was obtained during the induction period and at the beginning of the propenol formation in the gas phase; the spectrum (3) corresponds to the period of high propenol formation rate; the spectrum (4) shows the surface composition of the fully deactivated surface. The feasible structures of identified surface species – both spectators and the reaction intermediate – are shown on the right.

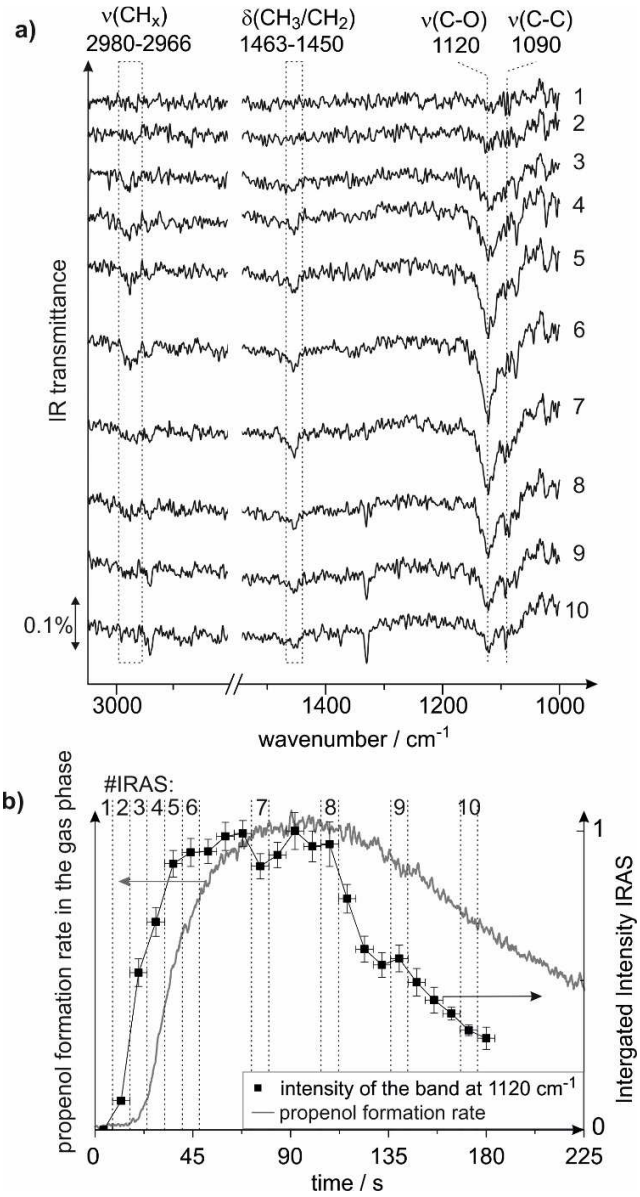

Figure 5: The correlation between the formation rate of the reaction intermediate RI on the surface and the evolution of propenol in the gas phase. (a) Series of IR spectra obtained over the Pd(111) surface turning over at 270 K under continuous exposure to acrolein and H_2. Shown are only the vibrational regions relevant to the reaction intermediate. The spectrum numbers correspond to the reaction times (indicated with dotted lines) that are shown in Fig.5(b); (b) The integrated intensity of the vibrational peak at 1120 cm^{-1} (black symbols) and the propenol formation rate in the gas phase (grey line) plotted as a function of reaction time. A clear correlation between the evolution of the reaction intermediate on the surface and propenol in the gas phase is observed.

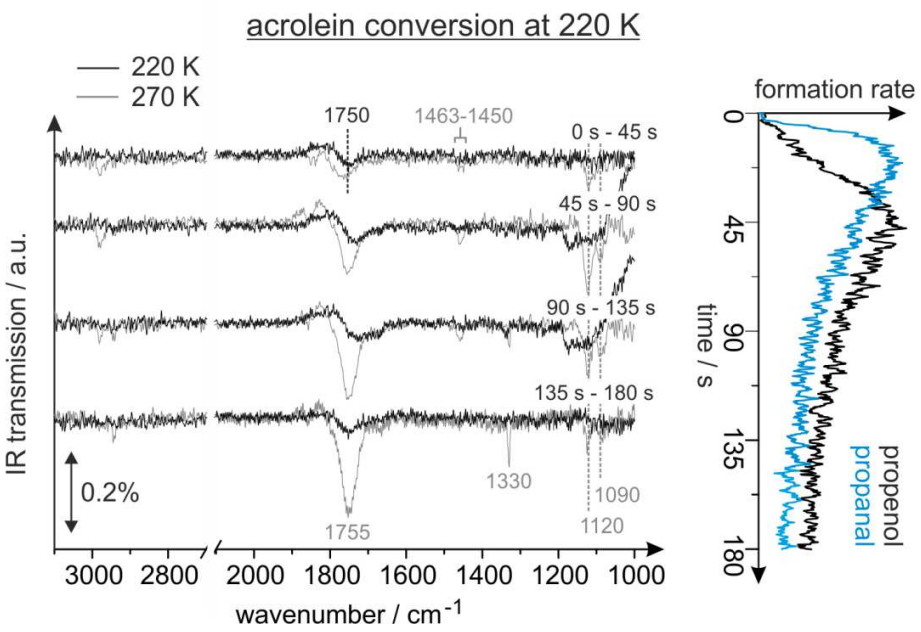

Figure 6: Production rate of the propanal and propenol on Pd(111) detected in the gas-phase (right) and the IRAS spectra recorded on the surface turning over at 220 K (left, black traces). The IRAS spectra obtained on the same surface at the reaction temperature 270 K are plotted together for comparison (grey traces).

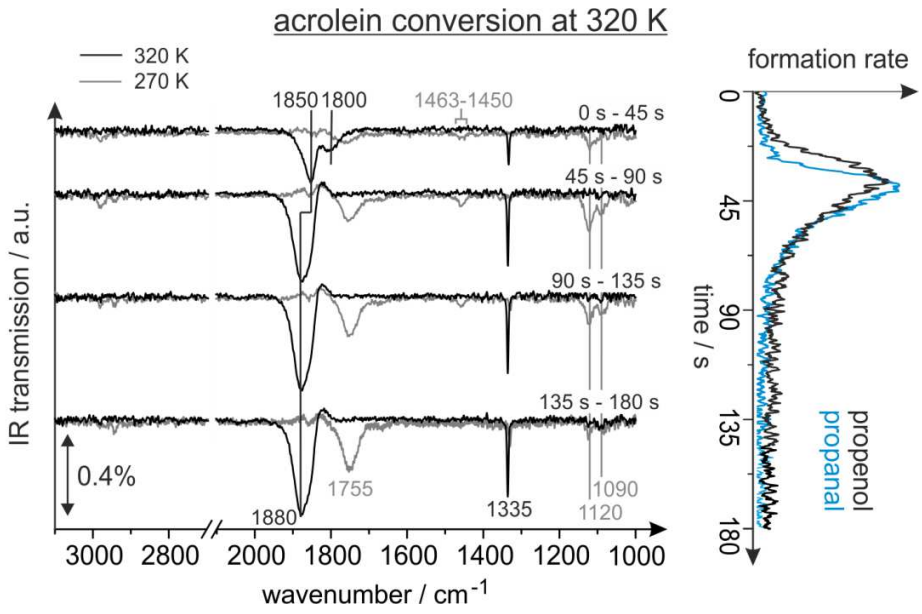

Figure 7: Production rate of the propanal and propenol on Pd (111) detected in the gas-phase (right) and the IRAS spectra recorded on the surface turning over at 320 K (left, black traces). The IRAS spectra obtained on the same surface at the reaction temperature 270 K are plotted together for comparison (grey traces).

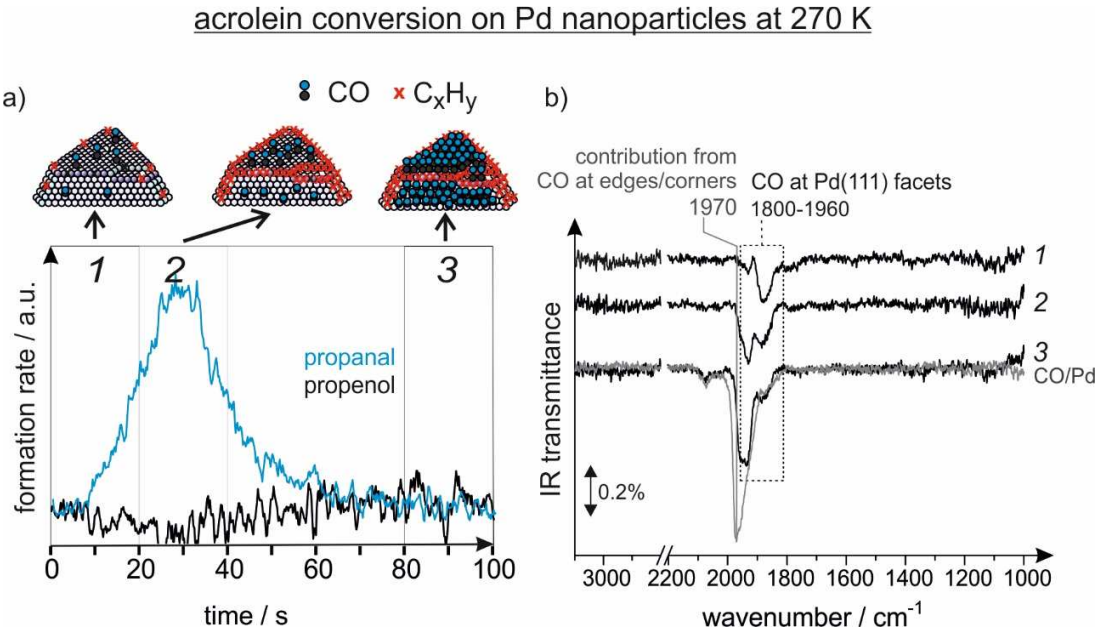

Figure 8: (a) Formation rates of propanal and propenol detected in the gas phase over 12 nm-sized Pd nanoparticles supported on Fe_3O_4/Pt(111) model film at 270 K and (b) simultaneously recorded IR spectra on this surface. The time resolution of the spectra is 20 s; the spectra 1 – 3 correspond to the regions 1 to 3 indicated in (a). The uppermost part of (a) shows the suggested model of the inhomogeneous accumulation of acrolein decomposition fragments (CO and CH_x).

References

1. (a) Gallezot, P.; Richard, D., Selective hydrogenation of alpha,beta-unsaturated aldehydes. *Catal. Rev.-Sci. Eng.* **1998,** *40* (1-2), 81-126; (b) Maki-Arvela, P.; Hajek, J.; Salmi, T.; Murzin, D. Y., Chemoselective hydrogenation of carbonyl compounds over heterogeneous catalysts. *Appl. Catal. A-Gen.* **2005,** *292*, 1-49; (c) Claus, P., Selective hydrogenation of ά,β-unsaturated aldehydes and other C=O and C=C bonds containing compounds. *Top. Catal.* **1998,** *5* (1-4), 51-62.
2. Mäki-Arvela, P.; Hájek, J.; Salmi, T.; Murzin, D. Y., Chemoselective hydrogenation of carbonyl compounds over heterogeneous catalysts. *Applied Catalysis A: General* **2005,** *292* (0), 1-49.
3. Birchem, T.; Pradier, C. M.; Berthier, Y.; Cordier, G., Hydrogenation of 3-Methyl-crotonaldehyde on the Pt(553) Stepped Surface: Influence of the Structure and of Preadsorbed Tin. *Journal of Catalysis* **1996,** *161* (1), 68-77.
4. Englisch, M.; Ranade, V. S.; Lercher, J. A., Hydrogenation of crotonaldehyde over Pt based bimetallic catalysts. *Journal of Molecular Catalysis A: Chemical* **1997,** *121* (1), 69-80.
5. (a) Marinelli, T. B. L. W.; Nabuurs, S.; Ponec, V., Activity and Selectivity in the Reactions of Substituted α,β-Unsaturated Aldehydes. *Journal of Catalysis* **1995,** *151* (2), 431-438; (b) Hutchings,

G. J.; King, F.; Okoye, I. P.; Padley, M. B.; Rochester, C. H., Selectivity Enhancement in the Hydrogenation of α, β-Unsaturated Aldehydes and Ketones Using Thiophene-Modified Catalysts. *Journal of Catalysis* **1994,** *148* (2), 453-463.
6. Pradier, C. M.; Birchem, T.; Berthier, Y.; Cordier, G., HYDROGENATION OF 3-METHYL-BUTENAL ON PT(110) - COMPARISON WITH PT(111). *Catal. Lett.* **1994,** *29* (3-4), 371-378.
7. (a) Vannice, M. A., The influence of MSI (metal–support interactions) on activity and selectivity in the hydrogenation of aldehydes and ketones. *Top. Catal.* **1997,** *4* (3-4), 241-248; (b) Englisch, M.; Jentys, A.; Lercher, J. A., Structure sensitivity of the hydrogenation of crotonaldehyde over Pt/SiO2 and Pt/TiO2. *Journal of Catalysis* **1997,** *166* (1), 25-35.
8. (a) Kliewer, C. J.; Bieri, M.; Somorjai, G. A., Hydrogenation of the α,β-Unsaturated Aldehydes Acrolein, Crotonaldehyde, and Prenal over Pt Single Crystals: A Kinetic and Sum-Frequency Generation Vibrational Spectroscopy Study. *Journal of the American Chemical Society* **2009,** *131* (29), 9958-9966; (b) Haubrich, J.; Loffreda, D.; Delbecq, F.; Sautet, P.; Krupski, A.; Becker, C.; Wandelt, K., Adsorption of α,β-Unsaturated Aldehydes on Pt(111) and Pt–Sn Alloys: II. Crotonaldehyde. *The Journal of Physical Chemistry C* **2009,** *113* (31), 13947-13967; (c) Kennedy, G.; Baker, L. R.; Somorjai, G. A., Selective Amplification of C□O Bond Hydrogenation on Pt/TiO2: Catalytic Reaction and Sum-Frequency Generation Vibrational Spectroscopy Studies of Crotonaldehyde Hydrogenation. *Angewandte Chemie International Edition* **2014,** *53* (13), 3405-3408; (d) de Jesús, J. C.; Zaera, F., Adsorption and thermal chemistry of acrolein and crotonaldehyde on Pt(111) surfaces. *Surf. Sci.* **1999,** *430* (1–3), 99-115; (e) Murillo, L. E.; Chen, J. G., A comparative study of the adsorption and hydrogenation of acrolein on Pt(1 1 1), Ni(1 1 1) film and Pt–Ni–Pt(1 1 1) bimetallic surfaces. *Surf. Sci.* **2008,** *602* (4), 919-931; (f) Loffreda, D.; Delbecq, F.; Vigné, F.; Sautet, P., Catalytic Hydrogenation of Unsaturated Aldehydes on Pt(111): Understanding the Selectivity from First-Principles Calculations. *Angewandte Chemie International Edition* **2005,** *44* (33), 5279-5282; (g) Ide, M. S.; Hao, B.; Neurock, M.; Davis, R. J., Mechanistic Insights on the Hydrogenation of α,β-Unsaturated Ketones and Aldehydes to Unsaturated Alcohols over Metal Catalysts. *ACS Catalysis* **2012,** *2* (4), 671-683.
9. Dostert, K.-H.; O'Brien, C. P.; Ivars-Barceló, F.; Schauermann, S.; Freund, H.-J., Spectators Control Selectivity in Surface Chemistry: Acrolein Partial Hydrogenation Over Pd. *Journal of the American Chemical Society* **2015,** *137* (42), 13496-13502.
10. Libuda, J.; Meusel, I.; Hartmann, J.; Freund, H. J., A molecular beam/surface spectroscopy apparatus for the study of reactions on complex model catalysts. *Review of Scientific Instruments* **2000,** *71* (12), 4395-4408.
11. (a) Weiss, W.; Ranke, W., Surface chemistry and catalysis on well-defined epitaxial iron-oxide layers. *Prog. Surf. Sci.* **2002,** *70* (1-3), 1-151; (b) Lemire, C.; Meyer, R.; Henrich, V. E.; Shaikhutdinov, S.; Freund, H. J., The surface structure of Fe3O4(111) films as studied by CO adsorption. *Surf. Sci.* **2004,** *572* (1), 103-114.
12. (a) Schalow, T.; Brandt, B.; Starr, D. E.; Laurin, M.; Schauermann, S.; Shaikhutdinov, S. K.; Libuda, J.; Freund, H. J., Oxygen-induced restructuring of a Pd/Fe3O4 model catalyst. *Catal. Lett.* **2006,** *107* (3-4), 189-196; (b) Schalow, T.; Brandt, B.; Starr, D. E.; Laurin, M.; Shaikhutdinov, S. K.; Schauermann, S.; Libuda, J.; Freund, H. J., Particle size dependent adsorption and reaction kinetics on reduced and partially oxidized Pd nanoparticles. *Phys. Chem. Chem. Phys.* **2007,** *9* (11), 1347-1361.
13. (a) Akita, M.; Osaka, N.; Itoh, K., Infra-red reflection absorption spectroscopic study on adsorption structures of acrolein on polycrystalline gold and Au(111) surfaces under ultra-high vacuum conditions. *Surf. Sci.* **1998,** *405* (2-3), 172-181; (b) Fujii, S.; Osaka, N.; Akita, M.; Itoh, K., INFRARED REFLECTION-ABSORPTION SPECTROSCOPIC STUDY ON THE ADSORPTION STRUCTURES OF ACROLEIN ON AN EVAPORATED SILVER FILM. *J. Phys. Chem.* **1995,** *99* (18), 6994-7001; (c) Hamada, Y.; Nishimura, Y.; Tsuboi, M., INFRARED-SPECTRUM OF TRANS-ACROLEIN. *Chem. Phys.* **1985,** *100* (3), 365-375; (d) Puzzarini, C.; Penocchio, E.; Biczysko, M.; Barone, V., Molecular Structure and Spectroscopic Signatures of Acrolein: Theory Meets Experiment. *J. Phys. Chem. A* **2014,**

118 (33), 6648-6656; (e) Loffreda, D.; Jugnet, Y.; Delbecq, F.; Bertolini, J. C.; Sautet, P., Coverage Dependent Adsorption of Acrolein on Pt(111) from a Combination of First Principle Theory and HREELS Study. *The Journal of Physical Chemistry B* **2004,** *108* (26), 9085-9093.
14. (a) Colthup, N. B.; Daly, L. H.; Wiberley, S. E., *Introduction to Infrared and Raman Spectroscopy*. 3rd ed.; Academic Press: San Diego and London, 1990; (b) Mecke, R.; Noack, K., UNTERSUCHUNGEN UBER DIE BEEINFLUSSUNG DER FREQUENZ UND INTENSITAT DER NU-C=O-BANDEN UND NU-C=C-BANDEN IM IR-SPEKTRUM UNGESATTIGTER KETONE DURCH KONJUGATION UND STERISCHE HINDERUNG. *Spectrochimica Acta* **1958,** *12* (4), 391-393; (c) Stein, S. E., In *NIST Chemistry WebBook, NIST Standard Reference Database Number 69*, Mallard, P. J. L. a. W. G., Ed. National Institute of Standards and Technology: Gaithersburg MD, August 1, 2014.
15. (a) Borasio, M.; de la Fuente, O. R.; Rupprechter, G.; Freund, H. J., In situ studies of methanol decomposition and oxidation on Pd(111) by PM-IRAS and XPS spectroscopy. *J. Phys. Chem. B* **2005,** *109* (38), 17791-17794; (b) Haubrich, J.; Loffreda, D.; Delbecq, F.; Sautet, P.; Jugnet, Y.; Krupski, A.; Becker, C.; Wandelt, K., Adsorption and vibrations of alpha,beta-unsaturated aldehydes on pure pt and Pt-Sn alloy (111) surfaces I. Prenal. *Journal of Physical Chemistry C* **2008,** *112* (10), 3701-3718; (c) Mitchell, W. J.; Xie, J.; Jachimowski, T. A.; Weinberg, W. H., CARBON-MONOXIDE HYDROGENATION ON THE RU(001) SURFACE AT LOW-TEMPERATURE USING GAS-PHASE ATOMIC-HYDROGEN - SPECTROSCOPIC EVIDENCE FOR THE CARBONYL INSERTION MECHANISM ON A TRANSITION-METAL SURFACE. *J. Am. Chem. Soc.* **1995,** *117* (9), 2606-2617; (d) Schauermann, S.; Hoffmann, J.; Johanek, V.; Hartmann, J.; Libuda, J., Adsorption, decomposition and oxidation of methanol on alumina supported palladium particles. *Physical Chemistry Chemical Physics* **2002,** *4* (15), 3909-3918; (e) Sexton, B. A., METHANOL DECOMPOSITION ON PLATINUM (111). *Surf. Sci.* **1981,** *102* (1), 271-281; (f) Davis, J.; Barteau, M., Polymerization and decarbonylation reactions of aldehydes on the Pd (111) surface. *J. Am. Chem. Soc.* **1989,** *111* (5), 1782-1792.
16. Haubrich, J.; Loffreda, D.; Delbecq, F.; Sautet, P.; Krupski, A.; Becker, C.; Wandeltt, K., Adsorption of alpha,beta-Unsaturated Aldehydes on Pt(111) and Pt-Sn Alloys: II. Crotonaldehyde. *Journal of Physical Chemistry C* **2009,** *113* (31), 13947-13967.
17. (a) Guirgis, G. A.; Drew, B. R.; Gounev, T. K.; Durig, J. R., Conformational stability and vibrational assignment of propanal. *Spectrochimica Acta Part a-Molecular and Biomolecular Spectroscopy* **1998,** *54* (1), 123-143; (b) Frankiss, S. G.; Kynaston, W., VIBRATIONAL-SPECTRA OF PROPANAL, 1-DEUTEROPROPANAL AND 2,2-DIDEUTEROPROPANAL. *Spectrochimica Acta Part a-Molecular Spectroscopy* **1972,** *A 28* (11), 2149-&.
18. (a) Hill, J. M.; Shen, J. Y.; Watwe, R. M.; Dumesic, J. A., Microcalorimetric, infrared spectroscopic, and DFT studies of ethylene adsorption on Pd and Pd/Sn catalysts. *Langmuir* **2000,** *16* (5), 2213-2219; (b) Mohsin, S. B.; Trenary, M.; Robota, H. J., KINETICS OF ETHYLIDYNE FORMATION ON PT(111) FROM TIME-DEPENDENT INFRARED-SPECTROSCOPY. *Chem. Phys. Lett.* **1989,** *154* (6), 511-515.
19. (a) Brown, N. F.; Barteau, M. A., REACTIONS OF UNSATURATED OXYGENATES ON RHODIUM(111) AS PROBES OF MULTIPLE COORDINATION OF ADSORBATES. *J. Am. Chem. Soc.* **1992,** *114* (11), 4258-4265; (b) de Jesus, J. C.; Zaera, F., Adsorption and thermal chemistry of acrolein and crotonaldehyde on Pt(111) surfaces. *Surf. Sci.* **1999,** *430* (1-3), 99-115; (c) de Jesus, J. C.; Zaera, F., Double-bond activation in unsaturated aldehydes: conversion of acrolein to propene and ketene on Pt(111) surfaces. *J. Mol. Catal. A-Chem.* **1999,** *138* (2-3), 237-240; (d) Davis, J. L.; Barteau, M. A., VINYL SUBSTITUENT EFFECTS ON THE REACTIONS OF HIGHER OXYGENATES ON PD(111). *Journal of Molecular Catalysis* **1992,** *77* (1), 109-124; (e) Haubrich, J.; Loffreda, D.; Delbecq, F.; Sautet, P.; Jugnet, Y.; Krupski, A.; Becker, C.; Wandelt, K., Mechanistic and spectroscopic identification of initial reaction intermediates for prenal decomposition on a platinum model catalyst. *Physical Chemistry Chemical Physics* **2011,** *13* (13), 6000-6009.
20. Christmann, K., Interaction of hydrogen with solid surfaces. *Surface Science Reports* **1988,** *9* (1–3), 1-163.

21. Hollins, P.; Pritchard, J., INFRARED STUDIES OF CHEMISORBED LAYERS ON SINGLE-CRYSTALS. *Prog. Surf. Sci.* **1985,** *19* (4), 275-350.
22. Hoffmann, F. M., Infrared reflection-absorption spectroscopy of adsorbed molecules. *Surface Science Reports* **1983,** *3* (2–3), 107-192.
23. Conrad, H.; Ertl, G.; Latta, E. E., Adsorption of hydrogen on palladium single crystal surfaces. *Surf. Sci.* **1974,** *41* (2), 435-446.
24. (a) O'Brien, C. P.; Dostert, K. H.; Hollerer, M.; Stiehler, C.; Calaza, F.; Schauermann, S.; Shaikhutdinov, S.; Sterrer, M.; Freund, H. J., Supports and modified nano-particles for designing model catalysts. *Faraday Discuss.* **2016**; (b) O'Brien, C. P.; Dostert, K.-H.; Schauermann, S.; Freund, H.-J., Selective Hydrogenation of Acrolein Over Pd Model Catalysts: Temperature and Particle-Size Effects. *Chemistry – A European Journal* **2016,** *22* (44), 15856-15863.
25. Ponec, V., On the role of promoters in hydrogenations on metals; alpha,beta-unsaturated aldehydes and ketones. *Appl. Catal. A-Gen.* **1997,** *149* (1), 27-48.
26. (a) Morkel, M.; Unterhalt, H.; Salmeron, M.; Rupprechter, G.; Freund, H.-J., SFG spectroscopy from 10−8 to 1000 mbar: less-ordered CO structures and coadsorption on Pd(1 1 1). *Surf. Sci.* **2003,** *532–535*, 103-107; (b) Unterhalt, H.; Rupprechter, G.; Freund, H.-J., Vibrational Sum Frequency Spectroscopy on Pd(111) and Supported Pd Nanoparticles: CO Adsorption from Ultrahigh Vacuum to Atmospheric Pressure†. *The Journal of Physical Chemistry B* **2002,** *106* (2), 356-367; (c) Bertarione, S.; Scarano, D.; Zecchina, A.; Johanek, V.; Hoffmann, J.; Schauermann, S.; Frank, M. M.; Libuda, J.; Rupprechter, G.; Freund, H. J., Surface reactivity of Pd nanoparticles supported on polycrystalline substrates as compared to thin film model catalysts: Infrared study of CO adsorption. *J. Phys. Chem. B* **2004,** *108* (11), 3603-3613; (d) Xu, X. P.; Goodman, D. W., AN INFRARED AND KINETIC-STUDY OF CO OXIDATION ON MODEL SILICA-SUPPORTED PALLADIUM CATALYSTS FROM 10-9 TO 15-TORR. *J. Phys. Chem.* **1993,** *97* (29), 7711-7718; (e) Goyhenex, C.; Croci, M.; Claeys, C.; Henry, C. R., FTIR studies of the adsorption of CO on supported metallic clusters PdMgO(100). *Surf. Sci.* **1996,** *352–354*, 475-479; (f) Francis, S. A.; Ellison, A. H., INFRARED SPECTRA OF MONOLAYERS ON METAL MIRRORS. *Journal of the Optical Society of America* **1959,** *49* (2), 131-138; (g) Wolter, K.; Seiferth, O.; Kuhlenbeck, H.; Bäumer, M.; Freund, H. J., Infrared spectroscopic investigation of CO adsorbed on Pd aggregates deposited on an alumina model support. *Surf. Sci.* **1998,** *399* (2–3), 190-198.
27. Yudanov, I. V.; Sahnoun, R.; Neyman, K. M.; Rösch, N.; Hoffmann, J.; Schauermann, S.; Johánek, V.; Unterhalt, H.; Rupprechter, G.; Libuda, J.; Freund, H.-J., CO Adsorption on Pd Nanoparticles: Density Functional and Vibrational Spectroscopy Studies. *The Journal of Physical Chemistry B* **2002,** *107* (1), 255-264.
28. Schauermann, S.; Hoffmann, J.; Johánek, V.; Hartmann, J.; Libuda, J.; Freund, H.-J., Catalytic Activity and Poisoning of Specific Sites on Supported Metal Nanoparticles. *Angewandte Chemie International Edition* **2002,** *41* (14), 2532-2535.